Optical Materials 142 (2023) 114055

Contents lists available at ScienceDirect

Optical Materials

journal homepage: www.elsevier.com/locate/optmat

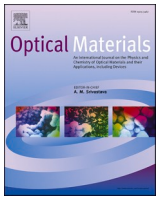

Near infrared laser irradiation on single multicellular spheroids

P. Camarero [a,b,c], P. Haro-González [a,c,d], M. Quintanilla [b,c,*]

[a] Nanomaterials for Bioimaging Group (NanoBIG), Universidad Autónoma de Madrid, Madrid, 28049, Spain
[b] Materials Physics Department, Universidad Autónoma de Madrid, Madrid, 28049, Spain
[c] Instituto de materiales Nicolás Cabrera (INC), Universidad Autónoma de Madrid, Madrid, 28049, Spain
[d] Institute for Advanced Research in Chemical Sciences, Universidad Autónoma de Madrid, Madrid, 28049, Spain

ARTICLE INFO

Keywords:
Multicellular tumor spheroid
Laser irradiation
Viability
Near infrared
Size change
Shrinking
Optical microscopy
Bioimaging

ABSTRACT

Light is being widely used in biomedicine due to its non-invasive nature, with application in imaging techniques and as a therapeutic agent. However, several aspects of its effect on irradiated tissues still leads to discussion in the scientific community. This particularly relates to novel biological models, as is the case of 3D multicellular spheroids, which are rising as an intermediate model between *in vitro* monolayer cultures and small animals. The applications of these spherical cell aggregates are diverse and include tissue reconstruction, drug testing or cancer studies, to cite some. To address the effect of light on these models, we use spheroids formed by MCF-7 (adenocarcinoma) or by U-87 MG (glioblastoma) cells. After their growth, they have been irradiated individually with focused laser radiation in the near-infrared (808 nm and 1450 nm), which provokes size changes in the spheroid. Time-lapse imaging in a brightfield microscope allows to define a reduction parameter, which informs about the extent of the size change. This parameter is correlated with cell viability studies; thus, we can set a safe range of reduction in which spheroids are not damaged by irradiation, and a threshold that should be avoided to keep cell mortality low. This correlation can be used as preliminary and visual information on the survival of cells during optical experiments with 3D spheroids.

1. Introduction

In the biomedical field, light is often used as a non-invasive way to interact with biological samples. If the energy that light carries is well controlled, it can be used for a wide gamut of techniques. The most straight forward ones are maybe those in which the outcome of the interaction is also light, which include options such as super-resolution and live cell imaging. However, light has also been proposed to trigger a therapeutic effect, as it happens in photoactivated chemotherapy, photoactivated drug delivery, and in photodynamic and photothermal therapies. Similarly, in the understanding of biological processes, light is a relevant tool thanks to techniques such as optogenetics, which has revolutionized neuroscience allowing an accurate control on the functions of specific cells. [1] Also in neuroscience, optical tweezers allow to manipulate whole neurons, as well as probing synapses and receptors. [2] The use of these techniques can be extended to characterize many different cells and tissues, provided that light can efficiently reach the target spot within the body, and that it doesn't produce any harm along the optical path. [1,3] Indeed, for the development of all these techniques, it is important to understand any side-effect that irradiation at a certain wavelength may have in the tissues.

The effect of light in tissues is a complex subject of discussion. While the cytotoxicity of ultraviolet light (up to 400 nm) is accepted without doubt, as it is known to be a carcinogen that triggers the production of reactive oxygen species and may initiate oxidative stress; visible light is often considered to be non-toxic. [4] Still, the accuracy of this claim depends on the irradiation dose (intensity and time), as biological tissues partially absorb visible light, subsequently increasing their temperature. Living organisms have very strict thermal requirements to live and proliferate. For instance, a mild thermal increase (reaching ~43 °C) can be used to weaken cancer cells, which constitutes an adjuvant treatment for chemotherapy and radiotherapy. If temperature is further enhanced, hyperthermia can be used as a stand-alone treatment killing affected cells. [5]

It seems clear that for all the techniques previously mentioned, irradiation doses must be carefully controlled to avoid overheating (or seeking it). The exact irradiation limit should depend on the wavelength of light, as light attenuation by tissues strongly depends on it. [6] The

Abbreviations: BW, Biological window.

* Corresponding author. Materials Physics Department, Universidad Autónoma de Madrid, Madrid, 28049, Spain.
E-mail address: marta.quintanilla@uam.es (M. Quintanilla).

https://doi.org/10.1016/j.optmat.2023.114055
Received 3 March 2023; Received in revised form 15 May 2023; Accepted 17 June 2023

study of the optical properties of different tissues has created a general frame on that regard, defining several spectral ranges in which light is attenuated to a lower extent, often called biological windows (BW). These ranges slightly vary between tissues but can be approximately identified as 650–950 nm (BW-I), 1000–1350 nm (BW-II), 1600–1870 nm (BW-III) and 2100–2300 nm (BW-IV). [7] Light within these ranges, all belonging to the near-infrared, deliver a lesser amount of heat to tissues and reaches deeper into them, hence a wavelength shift from the visible to the near-infrared is taking place in light-based biomedical tools. [8]

Light-based techniques for biomedicine are often developed to be used *in vivo*, thus light must interact with a highly complex and heterogeneous environment. This heterogeneity, together with the complexity of *in vivo* experiments, motivated the use of monolayer cell culture as a preliminary experimental step. This type of culture is traditionally used as *in vitro* test for the effect of drugs or external stimuli (temperature, radiation, pH) on healthy or cancer cells. If experiments are positive, *in vivo* experiments in animal models are typically carried out afterwards. However, *in vivo* experiments often show a very different experimental outcome compared to the one obtained *in vitro*. [11]

From the point of view of the cell environment the differences between the two models are many. In monolayer culture, being a 2D structure, the number of neighbouring cells is minimal. This reduces cell-cell interaction, including not only physical contact, but also intercell communication. From a geometric perspective, cells are spread on a plate where they stretch, presenting a differentiated cytoskeleton distribution and offering an increased surface to the medium. This modifies cell proliferation rates and improves their access to oxygen and nutrients, which in monolayer is thus only limited by the quality of the medium. This claim is also true regarding the concentration of debris and waste products in their direct environment. Instead, in a real tissue the microenvironment is defined by the vascular system, which forces a heterogeneous supply, being this a critical difference in the case of cancer tumors. Monolayer assays, though, provide preliminary information that helps reducing the use of animals, which is beneficial both from an economical and ethical perspective. In addition, they provide good reproducibility and control on the experiments, which is not easily achieved in *in vivo* situations.

In this context, the use of 3D cell culture has appeared as an intermediate option to bridge the gap between the two traditional models. 3D cell spheroids are aggregates of single or multiple cell lines which can be easily prepared *in vitro*, offering a high reproducibility through size and shape control. [9] Their 3D character improves the interaction between cells, promoting the production of extracellular proteins and improving inter-cell communication in a way that better resembles the one of cells in real tissues. In addition, a gradient of resources appears as one go deeper into the spheroid, as it happens in tissues due to the different distances to blood vessels. Taken to the extreme, though, this may become a limitation since 3D spheroids can develop a fully necrotic core. [9] Still, since this can be controlled through the age and size of spheroids, their use in the design of biological experiments is becoming more common. Specifically, it has been observed that they are closer to *in vivo* tissues than 2D cultures from the point of view of gene expression profiles, [10] response to thermal shock or thermotolerance, [11,12] signalling pathways, [9] or repair capability. [10]

Given the increased interest in near-infrared wavelengths, as well as in 3D spheroids, in this work we aim to settle a strategy to visually determine to what extent light can be damaging them. With this goal in mind, we have addressed the problem from the optics perspective, considering different treatments that deliver a different amount of energy. They include varying irradiation power, wavelength, and time. Regarding wavelengths, we consider the effect of 808 nm, belonging to the first biological window and often used in light-based therapies, and 1450 nm, which lies between the second and third BW and will serve as damage assay. Also, since each cell line has its own specific characteristics, which are translated to the spheroids, experiments include two model cell lines as an exploratory study. They have been chosen as limit cases regarding how their morphology determines the size of the spheroid, given by a very distinct intercellular space and thus, spheroid compactness. In particular, we have selected MCF-7, from epithelial breast cancer (adenocarcinoma) as dense spheroid, and U-87 MG, from epithelial brain cell (likely glioblastoma), which leaves a larger intercellular volume.

Experiments are performed in a brightfield optical microscope that allows for time-lapse imaging and thus shows the effect of light on the general appearance of the spheroid, and particularly on their size. As brightfield imaging is a technique that can be accessed in every laboratory working with cells, and size is an easily measurable parameter, its characterization can serve as a starting hint to determine the limiting irradiation dose a spheroid can stand. Thus, we are determining here the relationship between the observed size and a severe viability reduction.

2. Material and methods

2.1. Cell lines and culture conditions

Two cancer cell lines have been used: MCF-7 (Michigan Cancer Foundation-7) and U-87 MG (Uppsala 87 malignant glioblastoma). Both lines are derived from human epithelial tissue explants. Specifically, MCF-7 from breast human cancer (adenocarcinoma) and U-87 MG from brain human cancer (glioblastoma astrocytoma). These cell lines are selected due to their tendency to produce spheroids and because they present differentiated ways in which cells join. While MCF-7 cells form side-by-side junctions (Fig. 1(a)) that give rise to compact spheroids (Fig. 1(c)); U-87 MG present an elongated-shape with pseudopods (Fig. 1(b)), which constitute the links between cells, thus leading to less dense spheroids (Fig. 1(d)).

To produce 3D spheroids a standard monolayer culture is needed as source of cells. These cultures were routinely maintained in an incubator under the same conditions in 25 cm^3 flasks (Thermo Scientific) with Dulbecco's modified Eagle's medium (DMEM, Cytiva) supplemented with 10% Fetal Bovine Serum (Cytiva) and 1% Penicillin-Streptomycin (10,000 U/mL, HyClone).

2.2. Preparation of 3D multicellular spheroids

MCF-7 and U-87 MG spheroids were generated by forced floating method (Fig. 1(e)), a technique that provides highly reproducible spheroids. [13] The strategy is based in non-stick culture wells shaped to group the cells through gravity at the center. In this way, they adhere to each other, forming a sphere-like mass. To do so, a commercial round-bottom ultralow attachment well plate was used (ULA 96-well plate, Biofloat). To develop spheroids, 200 μL of complete culture medium with ~4000 cells is added to each well. The concentration of cells per mL was estimated using a Neubauer chamber, which is important in order to assure homogeneity between batches in the spheroids.

Prior to the experiments, the growth rate and morphology of the spheroids have been studied over 7 days (Fig. 1(f)), being day 0 the day in which culture starts. This study shows that spheroids are large and compact enough to be handled from day 2. With our culture conditions compactness happens spontaneously, without the need to apply any additional strategies such as the addition of collagen, which has been shown to be helpful in other works. [14] After day 4, a necrotic core becomes apparent in the spheroids. This agrees with the recent work of S.Rodrigues Alves et al., where the authors observed necrosis on day 4 and an increased percentage of apoptotic cells from day 4 to day 12. [15] Thus, we decided to irradiate them between the second and fourth days of growth. Typical diameters of the spheroids in this time frame are ~400 μm for U-87 MG and ~250 μm for MCF-7.

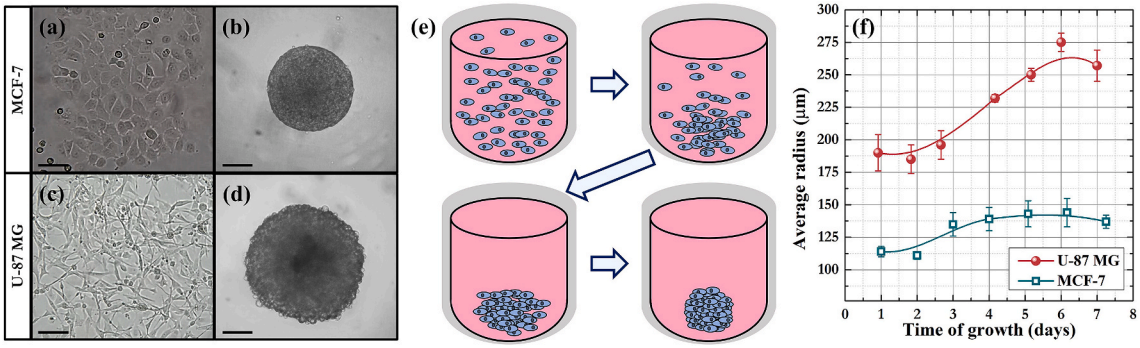

Fig. 1. Brightfield images of cells grown in monolayer culture showing their typical morphology ((a) and (c)), and example of the normal appearance of 3D spheroids ((b) and (d)) obtained with each cell line (MCF-7 in (a) and (b) and U-87 MG in (c) and (d)). A scheme of the evolution of 3D cultures is shown in (e). The first two illustrations occur on day 0, just after adding the cells to the well. In the third image (typically day 1) a spheroid already appears in the well, but it is not compact enough to be handled and easily breaks. The fourth image shows how spheroids appear during the following days. As preliminary test, the growth rate of spheroids has been monitored for both cell lines (n = 12 to 18) and is shown in (f). Scale bar: 100 μm.

2.3. Viability assays

After irradiation, each spheroid was collected with 40 μL of DMEM and transferred to a new round bottom plate. Additional 160 μL of fresh DMEM was then added to achieve optimal growth conditions, which were kept for 24 h in the incubator. In this way, healthy cells can reproduce, and damaged cells will die, facilitating the quantification of the extent of damage. Then, a commercial test (CellTiter-Glo 3D Cell Viability Assay, Promega) was used to assess viability. Its work is based on the luciferin-luciferase reaction that generates luminescence in the cells if they contain adenosine triphosphate (ATP). Briefly, the standard protocol includes to transfer the spheroids to 96-well plates with flat transparent bottom and opaque walls, add the commercial reagents, and then measure the luminescence intensity 20 min later. Light intensity was recorded using a plate reader (Synergy HTX, BioTek) that allows luminescence measurements. To transform this data into viability a negative control (untreated spheroids, n = 4, kept out of the incubator at the same time than the treated spheroids) is always included in the experiment, and its viability is used to define the 100%. An additional control with spheroids kept always in the incubator was done to assure that the time spent outside is not damaging them.

2.4. Irradiation of the spheroids

The experimental set-up shown in Fig. 2(a) has been used for the irradiation of the spheroids. First, spheroids are transferred from the 96-well plate to a sample holder specifically designed to hold them during treatment. Repeatability problems are emphasized when working with living biological samples. Thus, to keep error bars to a minimum, optical experiments need to be carefully designed. In our case, a 3D-printed resin mask (3D Creality Ender-3) was attached to a microscope glass slide. This mask (Fig. 2(a)) has a rectangular shape and eight circular wells, whose dimensions are chosen so they can contain enough culture medium to cover the spheroid (50 μL), but walls are low enough so light can be easily focused with the microscope objective (diameter of the well ~ 10 mm, height of the well ~ 2 mm). This design allows the spheroids to be individually trapped and irradiated in each well, and they are optically accessible to irradiate from above, and for imaging from below. In a single batch of measurements, half of the spheroids are irradiated, while the other half were used as viability control.

Power adjustable laser diodes are used as irradiation sources, collimated by a fiber port (PAF-X-7-C, Thorlabs) and focalized on the spheroid with a LWDPLAN microscope objective (10×, NA = 0.25). While the spheroid is irradiated, its brightfield image is recorded using an inverse microscope (Oxion, Euromex) that collects the image with a

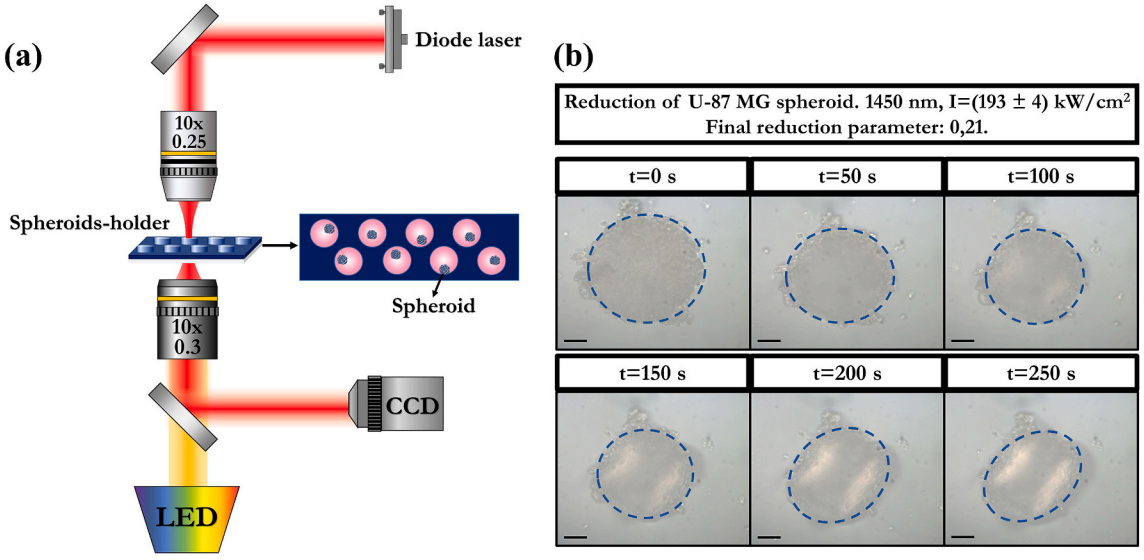

Fig. 2. Microscope design used to monitor spheroids (a) and time-lapse example of the images that can be obtained, which allow to study the evolution of spheroids (b). Blue discontinuous line marks the compact area of the spheroid, as used for its size measurement. Scale bar: 80 μm.

LMPLAN microscope objective (10×, NA = 0.3) and a CCD camera.

3. Results and discussion

Light irradiation is partially absorbed by cells thus its energy can be transformed into heat. Cells warmed up at temperatures beyond 40 °C may suffer health damage. Depending on the exact temperature and the length of the heat stress, they may recover afterwards or not. There are several ways in which cells may die, each accounting for different biomolecular processes and morphological changes. [16,17] The exact description of the processes resulting in their death depends on the strength of the insult, but also on the cell line and its living status at the moment of the stress. It is already settled that 3D spheroids show a better survival ratio to heat stress than monolayer cultures, though of course, heating may end up causing cellular death as well. [12] Previous reports have shown that heat shock may promote shrinkage or swelling of the spheroids during the next few days after treatment. [10] Also, it has been shown in a prostate cancer cell line (PC-3) that long treatments (>1 h) at low temperatures (43–45 °C) typically produce swelling, [18] same as shorter treatments (10 min) do in one of the cell lines used here (U-87 MG) when they reach temperatures above 53 °C caused by 808 nm light irradiation. [19] According to these previous works, both shrinkage or swallowing are mainly due to a disruption of cell organization and a consequent change of the intercellular space, being the effect stronger in the outer layers of cells. When mortality becomes high, cell death induces a reduction of cell adhesion and thus the spheroid swallows. [10,18]

Based on this information, our main goal is to determine whether it is possible to stablish a visual method to get a hint about cell damage during optical handling, which is useful when new experiments and therapeutic modes are designed. Optimally, the measured parameter must provide information at short irradiation times, so it becomes practical. In preliminary experiments monitoring spheroids irradiated with laser light in the optical microscope of Fig. 2(a), we have noted that in a short time (<100 s) spheroids visibly shrink (Fig. 2(b)). In some cases, specially related to MCF-7 spheroids, the harsher test treatments also produced swelling of the spheroid for irradiation times >100 s. This has been formerly linked to the expansion of the intercellular space and a complete death of the spheroid, [18,19] meaning that at this point irradiation dose is already too high for diagnostic or research techniques. Thus, we aim to focus on the first shrinking stage, as it may involve a reversible damage.

Aiming to compare the size of the spheroid over time and between samples, a reduction factor, R, has been defined as:

$$R = \frac{r_0 - r}{r_0} \tag{1}$$

where r_0 is the initial radium (at t = 0 s) and r is the radium measured in each frame. The chosen normalization by the initial radium allows to evaluate the extent of change independently of the initial size of the spheroid. This normalization is needed to avoid misinterpretations linked to the starting size because, even though the applied culture technique is providing highly homogeneous spheroids, there is still a certain degree of heterogeneity, especially when different cell lines are compared. This parameter is easily observable and measurable in any laboratory prepared to work with cells. However, *a priori*, it does not give us clear information about the living status of the spheroid after irradiation and requires calibration to evaluate its meaning in terms of cell survival.

To consistently determine the radium of the spheroids, r, we have considered that they are typically almost spherical (Fig. 1 (b) and (d)), but they are not perfect spheres. In addition, during treatment, thermal currents are formed that may move or rotate them, so different sides may be facing the camera and the same diameter cannot be measured always. For these reasons we have tested two methods to measure the radius: to calculate it from the average of several diameters, or to determine the area of the spheroid in the images and then calculate the corresponding radius of a circle with this area. Given the high sphericity of the spheroids, in our case both methods are giving almost the same results and could be used. Still, we have selected the strategy based on the area, judging that it can be also useful if spheroids are ill-shaped.

3.1. R as a function of time

To set a standard protocol for the experiments, we first address the size evolution of the spheroids over time. In order to do so, different irradiation doses were applied to the samples, varying both wavelength and power applied. The results obtained for both cell lines are shown in Fig. 3, in which the green band is indicated as a reference of the experimental error in the calculation of the reduction parameter (calculated as explained above).

From the figure, it is clear that there is a different response of the spheroids to each wavelength applied, as little or no change is observed upon irradiation at 808 nm (Fig. 3(a) and (b)), while there is a clear reduction when irradiation occurs at 1450 nm (Fig. 3(c) and (d)). For a fair comparison, it must be noted that the irradiation intensities considered are different for each wavelength, as the maximum power achieved is limited by the available laser diode. However, the power applied is higher for 808 nm, which is also the wavelength showing a smaller effect on reduction. Hence, the differential behavior of the spheroids is not related to the different irradiation dose, but to the wavelength.

A detailed inspection of the results obtained with irradiation at 1450 nm shows a steep initial slope in the reduction factor during the first 50 s of treatment, indicating a fast size reduction which hardly varies when both cell lines are compared (2,3% s^{-1} and 2,2% s^{-1} for the MCF-7 and U-87 MG spheroids, respectively, for the highest irradiation intensity). After this time, the change rate slows down, to the extent that for times longer than 150 s the spheroid stops changing size significantly. This seems to indicate that a saturation occurs in the reduction factor, which can be related to the fact that the spheroid must have a limit in the minimum size that each irradiation dose can provoke. Fig. 3(c) and (d) show that the maximum reduction is different for each cell line, which is consistent with their general characteristics. Since MCF-7 produces more compact spheroids, its maximum reduction factor must be smaller than that of U-87 MG, in which there is a larger volume of intercellular space prone to be eliminated. As mentioned earlier, the harshest treatment (and in a subtler way the previous one, at 193 kW/cm^2) end up inducing a swallow of MCF-7 spheroids for times >50s. Such effect has been previously linked to the complete death of the spheroid, and thus it should be avoided and won't be further studied here. However, it is interesting to note that this is not observed with equivalent treatments in U-87 MG cell line, which points out that compactness of the spheroid is a characteristic to consider in order to define the visual effect of irradiation doses. However, it must be noted that harsher treatments will probably provoke the same effect in U-87 MG cell line, though this is not tested here. [17]

The differences observed due to wavelength can be explained in terms of the laser-induced thermal increment, which is a consequence of the absorption of light by the sample at these wavelengths. Despite the presence of the cells, it can be approximated that the major component is cell medium (mostly water with some concentration of salts and proteins). In this case, the magnitude of the thermal increment can be determined by considering its absorption coefficient at each wavelength ($\alpha_{808} = 0.031 cm^{-1}$ and $\alpha_{1450} = 31.74\ cm^{-1}$, as measured) and the dimensions of the heating laser spot, following the method proposed by Mao et al. [20] Under our experimental conditions and assuming as thermal conductivity the one of water, the in-focus temperature increment can reach 60 °C (with room temperature at 20 °C) at 1450 nm, while it is negligible at 808 nm. Since a thermal increase that brings spheroids above 43 °C can already affect cellular functions, causing

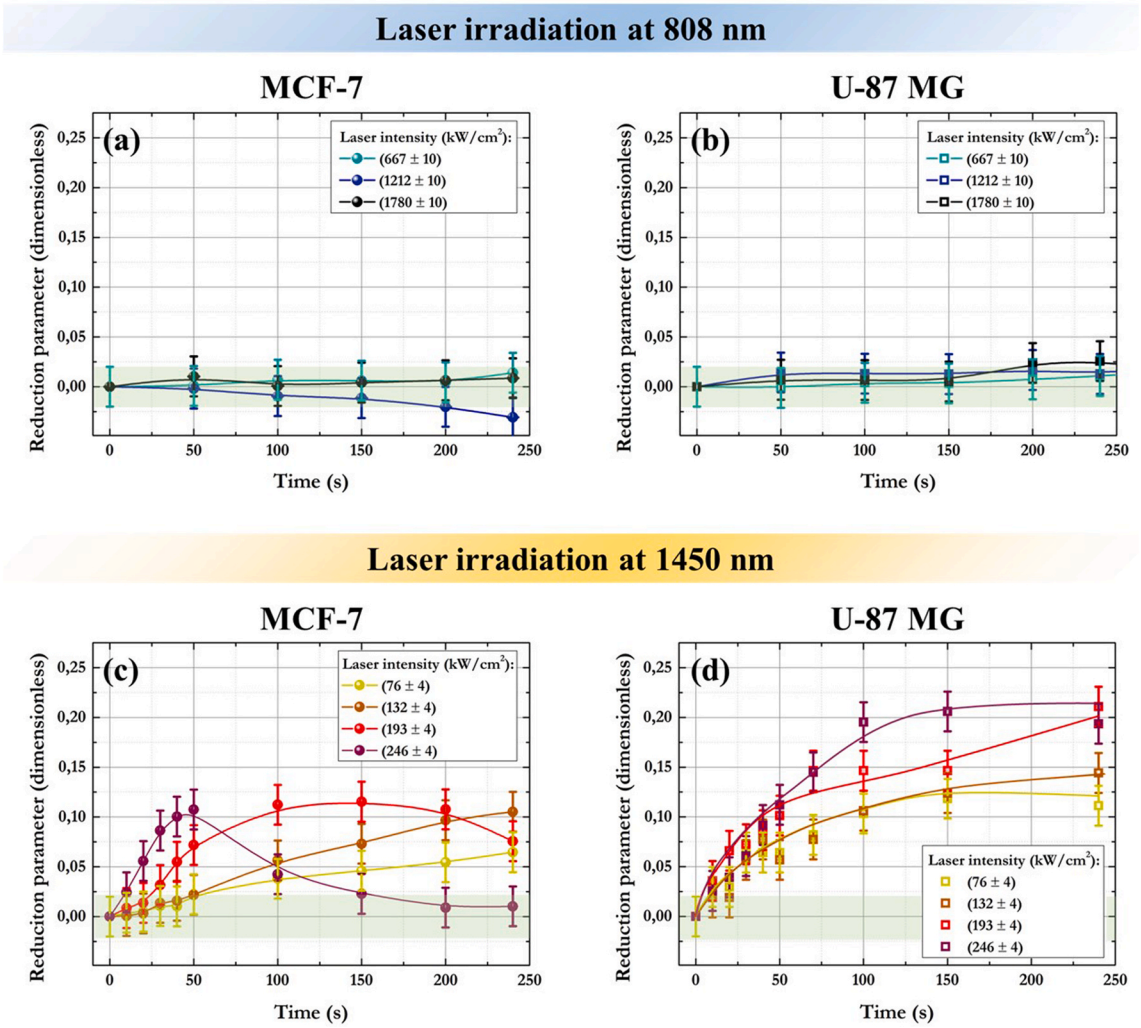

Fig. 3. Reduction parameter as a function of time at different laser intensities, with 808 nm for (a) MCF-7 and (b) U-87 MG cell lines, and with 1450 nm for (c) MCF-7 and (d) U-87 MG cell lines.

mortality, [16] it seems consistent that 1450 nm irradiation appears to be harsher than 808 nm. This increased absorption of cell media (and water) at 1450 nm is indeed the reason why this wavelength range is normally excluded from the biological windows. Still, the high temperature calculated rings an alarm related to the use of the second, third and fourth biological windows. In the wavelength range that covers BW-II, BW-III and BW-IV, scattering of biological tissues is lower than within the first BW, to the extent that even though water is absorbing in the whole range, the total optical extinction is low enough to shape the windows. [21,22] This makes this wavelength range relevant specifically in techniques in which spatial resolution needs to be good, as this is what low scattering allows. However, the results in Fig. 3 emphasize that light will be absorbed, and thus it is needed to pay attention to any symptoms of cell damage through overheating even within the windows.

To understand the situation in which the spheroid is during irradiation, it is important to underline that the calculated temperature refers to the focus spot only. Then, the thermal diffusivity of the medium will spread out heat, leading to the creation of a heat affected zone in the surroundings and altering a larger area of the spheroid. The extent of the damage depends not only on the final overall temperature, but also on the time this temperature is held and on the ability of the tissue to respond. Considering all these variables, it seems clear that to better quantify how harsh is a treatment, a cell viability study needs to be done. In order to do so, different treatments will be applied to the spheroids, seeking to obtain different R values, but all of them during 250 s, as at this time point the spheroids stopped shrinking.

3.2. *R as a function of the spheroid viability*

Fig. 4 shows the cellular viability as a function of the reduction factor, for the two cell lines treated and the two different laser wavelengths. The green band is indicated as reference value, corresponding to the experimental error committed in the calculation of the reduction parameter. The viability value of 80% is marked with a green horizontal line, as it is typically considered a reference value separating good viability of cells from damaged spheroids. Viability is defined as a percentage, being 100% the averaged viability of four spheroids left out of the incubator for the same time than irradiated spheroids. Spheroids, as living multicellular entities, cannot be identical to each other, which induces the data dispersion in viability observed in Fig. 4. Likely differences are, for instance, small inaccuracies in the number of starting cells, or the fact that in some cases spheroids are not perfect spheres, but they present groups of cells adhered to their surface (see, for instance, the spheroid in Fig. 2(b)). This outer cells may behave differently than the main spheroid body when irradiated, and produce dispersity in viability data.

Fig. 4(a) correspond to the results obtained irradiating MCF-7 spheroids, while U-87 MG results are plotted in Fig. 4(b). As it is expected, the irradiation at 808 nm (blue symbols) shows a viability above 80% for both cell lines, and size reduction, if any, is subtle, as it was

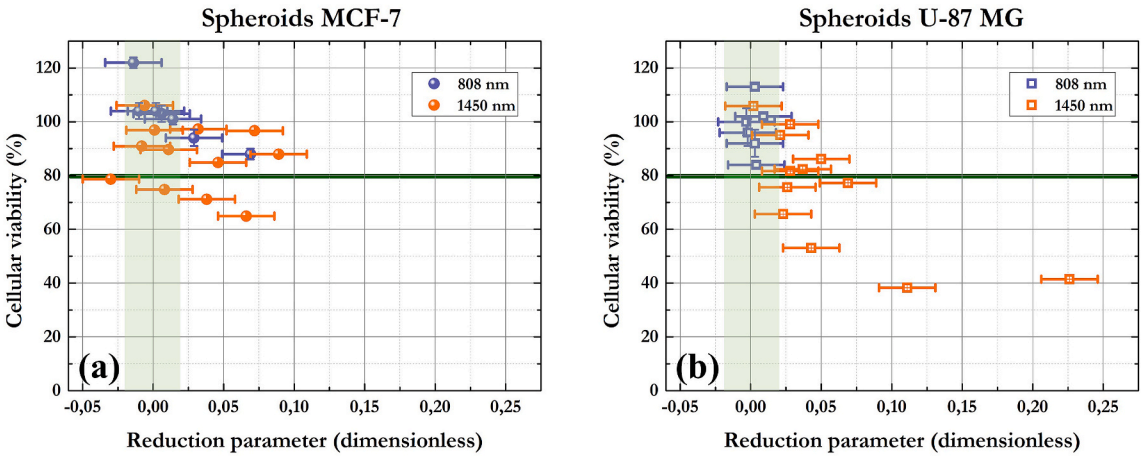

Fig. 4. Cell viability as a function of the reduction parameter for (a) MCF-7 and (b) U-87 MG cell lines, at 808 nm (blue dots) and 1450 nm (orange dots) irradiation wavelength. The horizontal green line marks the standard limit of cell viability, and the vertical green band marks the control area.

already shown in Fig. 3(a) and (b). This is consistent with the low heating created in these treatments. Instead, viability caused by treatments at 1450 nm may be in the range of damage, though not always, as was expected given the high temperatures that can be achieved in these experiments. The irradiation process in U-87 MG shows a clear decrease in the cell viability when R increases. It can be said that viability is typically high for $R < 0.025$, while if the reduction parameter lies between 0.025 and 0.075 viability might be compromised, but certainty cannot be provided. However, values of $R > 0.1$ must be clearly avoided if one needs to keep the spheroid alive (or they must be sought if mortality is a goal). In fact, the same observation applies to MCF-7, if it is considered that $R = 0.1$ was the prelude of spheroid swallowing (Fig. 3 (c)) which is in itself an indicative of cell death. Then, going back to Fig. 3(c) and (d), the maximum R threshold obtained would indicate that MCF-7 spheroids are slightly better standing irradiation, as the milder treatments did not reach this point.

Finally, it must be mentioned that the range of uncertainty ($0.025 < R < 0.075$) can be explained considering that multicellular models, as biological entities, always involve some differences between samples due to the initial status of cells (ageing of the culture, or live stage of cells). So even though they are prepared to be as homogeneous as possible, such data dispersion can be expected at intermediate treatments.

4. Conclusions

As seen, both cell lines have a distinct visual behavior towards the harsher irradiation doses in the near-infrared, which can be related to the starting volume of intercellular space and the temperature achieved in the spheroid. However, in the end, reduction factor and viability appear to be closely related: the lower the viability (greater cell death), the higher the reduction factor of the spheroid. Thus, size decrease upon irradiation can be used as an indicative of viability. In particular, values of R above 0.1 should be avoided as are indicative of a high mortality, while values between 0.025 and 0.75 represent an intermediate range of uncertainty. Smaller R values are typically related to high viability.

Of course, as the diversity of cell lines is huge and their preliminary health status may have consequences regarding survival, these conclusions cannot be considered as universal. Still, R remains as a good hint to start defining irradiation doses when an optical experiment with spheroids must be designed. This, we expect, can be particularly relevant as optical strategies in the biomedical field start exploring the low attenuation biological windows further in the near-infrared (BW-II to BW-IV). This claim is based on the fact that these windows are characteristic for very low tissue scattering, which is beneficial for a high spatial resolution and accuracy; but they also account for a higher light absorption than BW-I, and tissue might still be damaged through heating.

CRediT authorship contribution statement

P. Camarero: investigation, methodology, data curation, formal analysis, validation, writing (original draft) and visualization. P. Haro-González: supervision, conceptualization, writing (review & editing), project administration and funding acquisition. M. Quintanilla: supervision, conceptualization, methodology, resources, writing (original draft, review & editing).

Declaration of competing interest

The authors declare that they have no known competing financial interests or personal relationships that could have appeared to influence the work reported in this paper.

Data availability

Data will be made available on request.

Acknowledgements

The authors would like to acknowledge Dr. Malou Henriksen-Lacey and Prof. Luis Liz-Marzán, from CIC BiomaGUNE (San Sebastián, Spain), for supplying the cell lines.

Besides, we would like to mention our funding institution, Ministerio de Ciencia e Innovación de España (grants PID2019-105195RA-I00, PID2019-110632RB-I00, CNS2022-135495, CNS2022-135965 and TED2021-129937B-I00). P.C. thanks the regional government of Comunidad de Madrid for the Programa Investigo (Plan de Recuperación, Transformación y Resiliencia) which was developed thanks to SEPE, Ministerio de Trabajo y Economía Social and the European Union through NextGenerationEU.

References

[1] V. Emiliani, et al., Optogenetics for light control of biological systems, Nat. Rev. Methods Primers 2 (1) (2022) 55.
[2] I.C.D. Lenton, et al., Optical Tweezers Exploring Neuroscience 8 (2020).
[3] F. Català-Castro, E. Schäffer, M. Krieg, Exploring cell and tissue mechanics with optical tweezers, J. Cell Sci. 135 (15) (2022).
[4] S.L. Hopkins, et al., An in vitro cell irradiation protocol for testing photopharmaceuticals and the effect of blue, green, and red light on human cancer cell lines, Photochem. Photobiol. Sci. 15 (5) (2016) 644–653.

[5] J.C. Peeken, P. Vaupel, S.E. Combs, Integrating hyperthermia into modern radiation oncology: what evidence is necessary? Front. Oncol. 7 (2017) 132.
[6] J.F. Algorri, et al., Light Technology for Efficient and Effective Photodynamic Therapy: A Critical Review 13 (14) (2021) 3484.
[7] L.A. Sordillo, et al., Deep optical imaging of tissue using the second and third near-infrared spectral windows, J. Biomed. Opt. 19 (5) (2014), 056004.
[8] E. Hemmer, et al., Upconverting and NIR emitting rare earth based nanostructures for NIR-bioimaging, Nanoscale 5 (23) (2013) 11339–11361.
[9] S. Pozzi, et al., Meet me halfway: are in vitro 3D cancer models on the way to replace in vivo models for nanomedicine development? Adv. Drug Deliv. Rev. 175 (2021), 113760.
[10] S.C. Brüningk, et al., 3D tumour spheroids for the prediction of the effects of radiation and hyperthermia treatments, Sci. Rep. 10 (1) (2020) 1653.
[11] R. Gupta, D. Sharma, Therapeutic response differences between 2D and 3D tumor models of magnetic hyperthermia, Nanoscale Adv. 3 (13) (2021) 3663–3680.
[12] A.S. Song, A.M. Najjar, K.R. Diller, Thermally induced apoptosis, necrosis, and heat shock protein expression in 3D culture, J. Biomech. Eng. 136 (7) (2014).
[13] R.L.F. Amaral, et al., Comparative analysis of 3D bladder tumor spheroids obtained by forced floating and hanging drop methods for drug screening, Front. Physiol. 8 (2017) 605.
[14] I.R. Calori, et al., Type-I collagen/collagenase modulates the 3D structure and behavior of glioblastoma spheroid models, ACS Appl. Bio Mater. 5 (2) (2022) 723–733.
[15] S.R. Alves, et al., Characterization of glioblastoma spheroid models for drug screening and phototherapy assays, OpenNano 9 (2023), 100116.
[16] J.L. Roti Roti, Cellular responses to hyperthermia (40-46 degrees C): cell killing and molecular events, Int. J. Hyperther. 24 (1) (2008) 3–15.
[17] U. Ziegler, P. Groscurth, Morphological Features of Cell Death 19 (3) (2004) 124–128.
[18] P.N. Yi, et al., Swelling of multicellular spheroids induced by hyperthermia, Int. J. Hyperther. 3 (3) (1987) 217–233.
[19] M. Quintanilla, et al., Thermal monitoring during photothermia: hybrid probes for simultaneous plasmonic heating and near-infrared optical nanothermometry, Theranostics 9 (24) (2019) 7298–7312.
[20] H. Mao, et al., Temperature control methods in a laser tweezers system, Biophys. J. 89 (2005) 1308–1316.
[21] M. Quintanilla, et al., Challenges for optical nanothermometry in biological environments, Chem. Soc. Rev. 51 (11) (2022) 4223–4242.
[22] S.L. Jacques, Optical properties of biological tissues: a review, Phys. Med. Biol. 58 (11) (2013) R37–R61.